Light absorption engineering of hydrogenated nanocrystalline silicon by femtosecond laser

D. Q. Zheng,[1] Y. J. Ma,[1] L. Xu,[1] W. A. Su,[1] Q. H. Ye,[1] J. I. Oh,[1,2,3] and W. Z. Shen[1,*]

[1]*Laboratory of Condensed Matter Spectroscopy and Opto-Electronic Physics, Key Laboratory of Artificial Structures and Quantum Control (Ministry of Education), and Institute of Solar Energy, Department of Physics, Shanghai Jiao Tong University, 800 Dong Chuan Road, 200240 Shanghai, China*

[2]*Department of Physics, Boston College, Chestnut Hill, Massachusetts 02467, USA*

[3]*e-mail: ohje@bc.edu*

**Corresponding author: wzshen@sjtu.edu.cn*

Received May 23, 2012; revised June 29, 2012; accepted July 11, 2012; posted July 12, 2012 (Doc. ID 169140); published August 28, 2012

The light absorption coefficient of hydrogenated nanocrystalline silicon has been engineered to have a Gaussian distribution by means of absorption modification using a femtosecond laser. The absorption-modified sample exhibits a significant absorption enhancement of up to ~700%, and the strong absorption does not depend on the incident light. We propose a model responsible for this interesting behavior. In addition, we present an optical limiter constructed through this absorption engineering method. © 2012 Optical Society of America

OCIS codes: 140.3390, 160.1245, 190.4400, 230.4320.

Laser crystallization (LC) is an appealing technique by which to transform amorphous silicon into polycrystalline silicon, owing to the technique's high throughput and high-definition growth at low temperature. The underlying mechanism of LC has been well understood, owing to numerous studies using various laser setups, including continuous and pulsed (nanosecond, picosecond, and femtosecond) lasers [1–7]. LC has also been demonstrated to be a useful tool for electronic device applications, which, however, have been rather restricted to thin-film transistors [1–3] and solar cells [4] to date. Since LC can be expected to lead to certain changes in the absorption properties of subject samples, it is of importance to investigate such optical aspects of LC-modified materials.

Recently, we demonstrated highly tunable nonlinear absorption (NLA) in hydrogenated nanocrystalline silicon (nc-Si:H), comprising silicon nanocrystallites embedded in an amorphous Si:H matrix [8]. Here we show that the absorption coefficient of nc-Si:H can be further engineered to be spatially dependent through the LC process using a femtosecond laser, after which nc-Si:H exhibits significantly strong NLA. We also propose a model to explain this laser-induced NLA. Moreover, we demonstrate that this absorption-engineering technique can be applied to the development of an optical limiter.

We used plasma-enhanced chemical vapor deposition to grow nc-Si:H thin films on glass substrates. We then made physical characterizations with x-ray diffraction and high-resolution transmission electron microscopy (nanocrystalline size d), Raman spectroscopy (crystalline volume fraction X_c), and optical transmission measurements (film thickness L, energy bandgap E_g, and absorption coefficient α). Detailed growth conditions and physical characterizations can be found in our previous work [8,9]. The physical parameters of the nc-Si:H in this work are summarized as $d \sim 6.0$ nm, $X_c \sim 43\%$, $L \sim 1.0$ μm, and $E_g \sim 1.60$ eV and with α as presented in Fig. 2(d) below.

For the femtosecond LC and Z-scan measurements, performed at ambient temperature and pressure, we used a mode-locked Ti:sapphire laser (Spectra-Physics 3960d-X3S) with 500 mW output power, generating Gaussian-shaped pulses of TEM_{00} spatial mode, 100 fs duration, 82 MHz repetition rate, and tunable wavelength ($\lambda = 770$–810 nm). The pulses were focused with a lens of 75 mm focal length, and the beam waist was ~25.5 μm. A lock-in amplifier (PerkinElmer 7265) was used to regulate the light chopper at 1 kHz, turning a train of 41,000 pulses on for 0.5 ms and off for the next 0.5 ms. In order for the nanosecond LC to produce large crystallized areas of constant X_c, we used a XeCl excimer laser, operated at $\lambda = 308$ nm and 10 Hz repetition rate, generating 20 ns single pulses of high energy density (50–600 mJ/cm^2). Before irradiating the sample, the Gaussian-shaped beams were passed through a homogenizer to change into flat-topped square-shaped beams of ~2.0 mm × 2.5 mm. We stepped the laser system in a 5×4 array with the sample at a fixed position in vacuum at ambient temperature, yielding a ~1.0 cm × 1.0 cm crystallized area.

We present in Fig. 1(a) the I_0-dependent open-aperture (OA) Z-scan transmittance spectra of the sample at

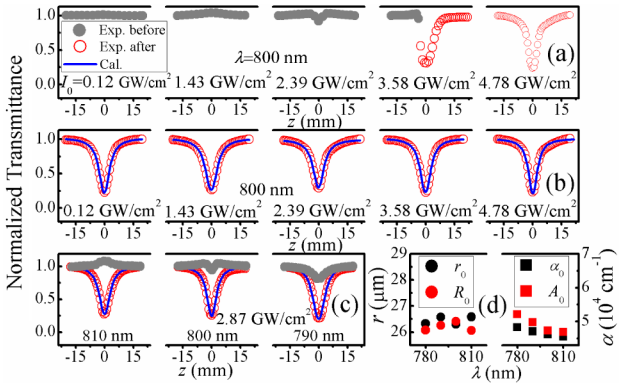

Fig. 1. (Color online) I_0-dependent OA Z-scan curves at $\lambda = 800$ nm. (a) Evolution of an absorption modification and (b) NLA behavior after the absorption modification; and λ-dependent (c) OA Z-scan curves at $I_0 = 2.87$ GW/cm^2 and (d) absorption parameters, (r_0, α_0) and (R_0, A_0).

$\lambda = 800$ nm, where I_0 is the irradiance of the incident laser pulses at focus (i.e., $z = 0$), excluding Fresnel reflection loss [10]. As I_0 varies from 0.12 to 2.39 GW/cm^2, the sample shows the NLA switching behavior from saturable absorption (SA) to reverse saturable absorption (RSA), as fully discussed in [8]. At a higher irradiance of $I_0 = 3.58$ GW/cm^2, on the other hand, there occurs an absorption jump after which the absorption properties are clearly changed, attributable to LC as discussed below. The absorption-modified sample exhibits a significant absorption enhancement (i.e., transmittance reduction), e.g., ~700% enhancement at $z = 0$ for $I_0 = 4.78$GW/cm^2 over that at $I_0 = 2.39$GW/cm^2. It also exhibits interestingly different absorption behaviors as shown in Fig. 1(b), where we present Z-scan curves obtained under the same conditions as in Fig. 1(a) after the absorption modification. The absorption-modified sample shows only RSA but no SA, and these strong RSA signals have almost no I_0 dependence.

We also present, in Fig. 1(c), λ-dependent OA Z-scan curves at $I_0 = 2.87$ GW/cm^2 before and after the absorption modification occurs. Before it does, the sample shows the λ-driven NLA switching, as also discussed in [8]. After it occurs, on the other hand, the sample displays very strong RSA signals. These strong NLA signals have almost no λ dependence. Thus, we come to the conclusion that the NLA signal of nc-Si:H can be engineered through this absorption modification to be significantly strong and insensitive to the incident light.

To better understand the absorption modification, we first used an optical microscope to inspect the absorption-modified sample. As shown in Fig. 2(a), we observed a ring pattern, which typically occurs when a silicon surface is irradiated by laser pulses [7]: ablation at the central spot, modification (oxidation/amorphization) along the outer ring, and annealing between them. The mechanisms of these laser-induced structural changes in silicon materials have been well studied in detail and can be found in the literature (e.g., [7]). Here we focus our attention only on the physical mechanism responsible for the observed NLA signals after the absorption modification. We employed micro-Raman spectroscopy to perform 20×20 matrix mapping, yielding 400 Raman spectra, over an area of 60 μm $\times$ 60 μm. We then calculated the two-dimensional X_c distribution [11], as presented in Fig. 2(b). The dark gray background (blue online) has $X_c \sim 43\%$, indicative of the starting nc-Si:H sample. The central core (red), corresponding to the laser ablation region, has an extremely high X_c (over 90%). Between these areas, there exists a ring (greenish), including the annealing and modification (oxidation/amorphization) regions, whose X_c gradually varies along the radial direction. Thus, the absorption-modified sample can be manifested solely by X_c, and the absorption modification appears to be caused by LC gradient, likely leading to the spatially dependent absorption coefficient, $\alpha(r)$.

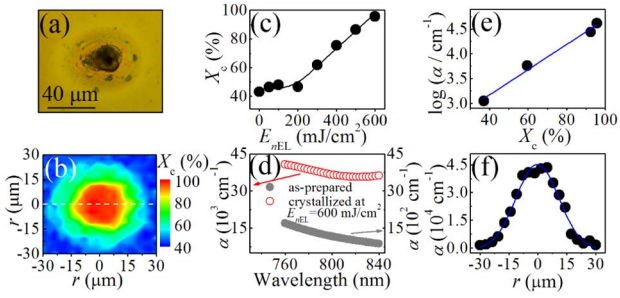

Fig. 2. (Color online) (a) Optical microscope image after the absorption modification; (b) two-dimensional X_c distribution; (c) X_c versus $E_{n\mathrm{EL}}$; the line is to guide the eye; (d) wavelength-dependent absorption coefficients for the as-prepared and crystallized nc-Si:H samples; (e) logarithmic absorption coefficient versus X_c at $\lambda = 800$ nm; the solid line is a linear fit; (f) absorption coefficient of the absorption-modified spot along the dashed line in (b), deduced from (e); the solid line is a Gaussian fit.

Currently, there appears to be a lack of technology to directly measure such spatially dependent $\alpha(r)$, especially on small areas. To estimate $\alpha(r)$, we hence used a nanosecond excimer laser to gain large crystallized areas, each of which has the 1.0 cm $\times$ 1.0 cm area and a constant X_c. In Fig. 2(c), we present X_c as a function of the energy density of the excimer laser ($E_{n\mathrm{EL}}$), from which the threshold $E_{n\mathrm{EL}}$ of LC can be found to be ~200 mJ/cm^2, consistent with previously reported values in silicon materials [3,12]. Note that this threshold value can be considered the effective energy density at the circular boundary between the background (blue) and annular (greenish) areas in Fig. 2(b). The large crystallized area of constant X_c allowed us to measure the λ-dependent transmission spectrum, which was performed with an n&k Technology Analyzer 1280 spectrophotometer. The absorption coefficient was then extracted from the transmission spectrum as in Fig. 2(d), where we show only a representative sample crystallized at $E_{n\mathrm{EL}} = 600$ mJ/cm^2 and the as-prepared nc-Si:H sample for comparison. One can see from the figure that the absorption coefficient is an order of magnitude larger for the crystallized than for the as-prepared nc-Si:H, clearly explaining the significant absorption enhancement of the absorption-modified sample. The absorption coefficient of the crystallized sample can be expressed in terms of X_c for a given λ from Figs. 2(c) and 2(d). We show in Fig. 2(e) the case for $\lambda = 800$ nm, yielding $\log \alpha(\mathrm{cm}^{-1}) = C_0 + C_1 X_c(\%)$ $(C_0 = 2.15, C_1 = 2.55 \times 10^{-2})$. With this, $\alpha(r)$ can be readily estimated as presented in Fig. 2(f), and its functional form can be found as

$$\alpha(r) = \alpha_a + \alpha_0 \exp\left(-\frac{2r^2}{r_0^2}\right), \tag{1}$$

where α_a is the absorption coefficient of the as-prepared nc-Si:H and α_0 and r_0 are deduced absorption parameters for the absorption-modified spot from the results of nanosecond LC, whose λ dependence is presented in Fig. 1(d).

Here we propose a model to explain the observed NLA signals after the absorption modification. At a given λ, the differential equation governing the absorption of light in the nc-Si:H sample can be written as

$$\frac{dI}{dz'} = -\alpha I = -\left[\alpha_a + A_0 \exp\left(-\frac{2r^2}{R_0^2}\right) + \alpha(I)\right] I, \tag{2}$$

where I is the beam irradiance, z' is the propagation depth into the sample, and α is the total absorption coefficient. The first term, α_a, a constant absorption

coefficient of the as-prepared nc-Si:H, characterizes the linear absorption. The second term, in the form of a Gaussian distribution, controls nonlinear absorption with respect to the space parameter r, which is a key of our model, and the last term does the same with respect to the irradiance. Note that A_0 and R_0, which are methodologically different from a_0 and r_0 in Eq. (1), will be determined from the Z-scan results in Figs. 1(b) and 1(c), whereas the last term is essentially same as the nonlinear absorption coefficient governing the SA-to-RSA absorption switching, as described in [8]. More importantly, the last nonlinear absorption term can be ignored in the absorption-modified spot, since its contribution to the total absorption clearly diminishes after the absorption modification, as can be seen in Fig. 1, resulting in an obvious solution of the differential equation. Now the transmittance at a sample position z for an OA Z scan can be expressed as [10]

$$T(z) = \frac{\int_{-\infty}^{+\infty} \mathrm{d}t \int_0^{+\infty} I_{\mathrm{out}} r \mathrm{d}r}{e^{-\alpha_a L} \int_{-\infty}^{+\infty} \mathrm{d}t \int_0^{+\infty} I_{\mathrm{in}} r \mathrm{d}r} = \frac{4}{w_z^2} \int_0^{\infty} e^{-(2r^2/w_z^2) - A_0 \exp(-2r^2/R_0^2) L} r \mathrm{d}r, \quad (3)$$

where I_{in} is the Gaussian-shaped input irradiance, I_{out} is the output irradiance that is the solution of Eq. (2), L is the sample thickness, $w_z^2 = w_0^2(1 + z^2/z_0^2)$ is the beam radius, w_0 is the beam waist, $z_0 = kw_0^2/2$ is the diffraction length of the laser beam, and $k = 2\pi/\lambda$ is the wave vector. As can be seen in Figs. 1(b) and 1(c), the calculated transmittance (solid lines) evidently fits the observed Z-scan results (circles), indicating that our model well explains the NLA signals after the absorption modification. As can also be seen in Fig. 1(d), the absorption parameters (A_0, R_0) of the absorption-modified spot obtained from the fitting of experimental Z-scan curves are in good agreement with those [(α_0, r_0)] deduced from the results of the nanosecond LC, indicating the validity of the indirect measurement of $\alpha(r)$ for the absorption-modified spot in Fig. 2(f). It is worth noting that we measured an OA Z-scan curve for the nanosecond laser crystallized sample at 600 mJ/cm^2 that is nearly flat (not shown), implying that the NLA signals after the absorption modification result from the Gaussian aspect of X_c, but not from changes of the bandgap or the optical properties in a highly crystallized sample.

Finally, we discuss an optical unit easily constructed from the absorption-modified nc-Si:H sample with carbon disulfide (CS_2), as shown in the inset of Fig. 3(a). An absorption-modified spot of ~50 μm diameter was obtained using the femtosecond laser with $I_0 = 4.78$ GW/cm^2; CS_2, which was kept in a quartz cuvette of 1 mm thickness, is a standard nonlinear refractive solvent having a strong Kerr effect [10,13]; and the distance between them was kept at 5 cm. The power-dependent transmittance of the incident laser in Fig. 3(a) clearly demonstrates that the optical unit exhibits optical limiting behavior, with a cutoff power of ~100 mW. This behavior clearly results from the interplay between the CS_2 cell and the absorption-modified sample. The CS_2 shows no nonlinear absorption, as seen from the OA Z-scan curve (almost flat) in Fig. 3(b), indicating that CS_2 itself will not lead to such optical limiting. On the other hand, it has a Kerr-induced self-focusing effect, as seen from the closed–aperture (CA) Z-scan curve (valley–peak shape) in the figure. Thus, as the power increases the laser beam is more and more focused on the absorption-modified spot so that the RSA effect of the spot becomes visible after a certain power, which is ~100 mW for our optical limiter.

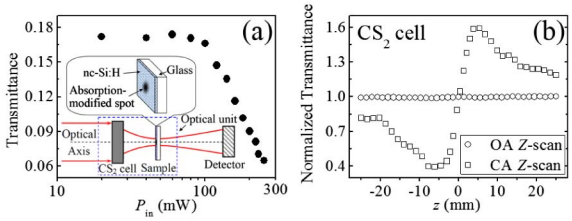

Fig. 3. (Color online) (a) Transmittance of an optical unit as a function of power of an incident laser beam at $\lambda = 800$ nm, demonstrating optical limiting behavior; the inset shows a schematic drawing of the experimental setup; (b) OA and CA Z-scan curves of CS_2 at $\lambda = 800$ nm and $I_0 = 5.97$ GW/cm^2.

In summary, we have shown that the absorption coefficient of nc-Si:H can be engineered to have a Gaussian distribution by means of femtosecond-laser-induced absorption modification. The absorption-modified nc-Si:H sample shows incident-light-independent, very strong RSA signals, and we find that such interesting NLA signals are well described by our proposed model. We have also demonstrated that this absorption engineering technique can be utilized to build an optical limiter.

We acknowledge Professor M. J. Naughton (Boston College) for beneficial suggestions on preparation of the manuscript. This work was supported by the National Major Basic Research Project (2012CB934302) and the National Natural Science Foundation (11074169 and 11174202) of China.

References

1. T. Sameshima, S. Usui, and M. Sekiya, IEEE Electron Device Lett. **7**, 276 (1986).
2. S. Brotherton, D. McCulloch, J. Clegg, and J. Gowers, IEEE Trans. Electron Devices **40**, 407 (1993).
3. T. Pier, K. Kandoussi, C. Simon, N. Coulon, H. Lhermite, T. Mohammed-Brahim, and J.-F. Bergamini, Thin Solid Films **515**, 7585 (2007).
4. A. Adikaari, N. Mudugamuwa, and S. Silva, Sol. Energy Mater. Sol. Cells **92**, 634 (2008).
5. H. Mavi, A. Shukla, S. Abbi, and K. Jain, J. Appl. Phys. **66**, 5322 (1989).
6. D. Von der Linde and N. Fabricius, Appl. Phys. Lett. **41**, 991 (1982).
7. J. Bonse, S. Baudach, J. Krüger, W. Kautek, and M. Lenzner, Appl. Phys. A **74**, 19 (2002).
8. Y. J. Ma, J. I. Oh, D. Q. Zheng, W. A. Su, and W. Z. Shen, Opt. Lett. **36**, 3431 (2011).
9. L. Xu, Z. P. Li, C. Wen, and W. Z. Shen, J. Appl. Phys. **110**, 064315 (2011).
10. M. Sheik-Bahae, A. A. Said, T. H. Wei, D. J. Hagan, and E. W. Van Stryland, IEEE J. Quantum Electron. **26**, 760 (1990).
11. E. Bustarret, M. Hachicha, and M. Brunel, Appl. Phys. Lett. **52**, 1675 (1988).
12. Z. Yuan, Q. Lou, J. Zhou, J. Dong, Y. Wei, Z. Wang, H. Zhao, and G. Wu, Opt. Laser Technol. **41**, 380 (2009).
13. P. Thomas, A. Jares, and B. Stoicheff, IEEE J. Quantum Electron. **10**, 493 (1974).